Far East Journal of Electronics and Communications

http://www.pphmj.com
http://dx.doi.org/10.17654/0973700622003
Volume 26, 2022, Pages 17-32 **P-ISSN: 0973-7006**

CIRCULARLY POLARIZED METAMATERIAL PATCH ANTENNA CIRCUITRY FOR MODERN APPLICATIONS

Marwah Haleem[1] **and Taha A. Elwi**[2,3]

[1]Department of Information and Communication Engineering
College of Information Engineering
Al-Nahrain University
Iraq

[2]Communication Engineering Department
Al-Ma'moon University College
Baghdad, Iraq

[3]International Applied and Theoretical Research Center (IATRC)
Baghdad Quarter, Iraq

Abstract

The proposed antenna structure is designed for modern wireless communication systems. The antenna structure is consistent with twelve-unit metamaterial (MTM) unit cells. Therefore, the antenna size is miniaturized effectively to $30 \times 40 \text{mm}^2$ which is equivalently

Received: September 4, 2022; Accepted: October 13, 2022

Keywords and phrases: twelve-unit metamaterial (MTM) unit cells, Hilbert shape MTM structure, T-resonator induction structure

How to cite this article: Marwah Haleem and Taha A. Elwi, Circularly polarized metamaterial patch antenna circuitry for modern applications, Far East Journal of Electronics and Communications 26 (2022), 17-32. http://dx.doi.org/10.17654/0973700622003

Published Online: December 15, 2022

about $0.2\lambda_0$, where λ_0 is the free space wavelength at 2.7GHz. This is achieved by conducting the use of Hilbert shape MTM structure with T-resonator induction structure. The antenna structure is printed on a single side substrate to cover the frequency bands from 2.7GHz to 3.7GHz and 5.4GHz to 5.6GHz. Such antenna is found to provide a maximum gain of 2.2dBi at first and the second band of interest. Next, proposed antenna is found to be circularly polarized at 3.3GHz and 5.6GHz. The proposed antenna performance is simulated numerically using CST MWS software package with all design methodology that is chosen to arrive to the optimal performance. Then, the optimal antenna design is tested numerically using HFSS software package for validation. Finally, an excellent agreement is achieved between the two conducted software results.

I. Introduction

Due to the recent growth in modern communication systems, several requirements are demanded to satisfy the current state of the arts in the antenna design [1]. The emergence and development of the concept of artificial materials throughout years led to a revolution microwave researches [1]. So, an antenna is an element of a cellular transmission line and is one of the most critical components of wireless communications systems. Dipoles/monopoles, slot/horn antennas, loop antennas, microstrip antennas, reflector antennas, helical antennas, dielectric/lens antennas, log periodic antennas and frequency-independent antennas are nine different kinds of antennas that have been developed in the last fifty years for both communication and navigation systems. Each type is better suited to a specific application than the others. Because of its low cost, light weight, and ease of fabrication, microstrip antennas are the most commonly used in reconfigurable antenna designs [2].

The idea of reconfigurable antennas can be traced back to a D. Schubert patent from 1983 [2]. In 1999, the United State Defense Advanced Research Projects Agency (DARPA) funded a project called “Reconfigurable Aperture Program (RECAP)” to look into the subject in applications of

reconfigurable antennas [3]. Reconfigurable antennas have also been used in applications such as broadband networking, cognitive radio, MIMO systems, and others.

So, changing the frequency, polarization, or radiation characteristics of an antenna may be used to reconfigure it. The majority of antenna reconfigurability techniques redistribute antenna currents, changing the electromagnetic fields of the antenna's efficient aperture [4]. Recently, reconfigurable patch antennas are the most commonly produced reconfigurable style antennas due to the ease of fabrication and incorporation into small electronic devices such as mobile phones and laptops. A standard reconfigurable patch antenna is made up of several separate metalized regions that are carried out on a plane and connected through switches or tuning components [4]. Different metalized parts can be brought in contact with each other by dynamically regulating the state of the switches, thus altering the overall antenna's radiation efficiency [5].

However, antennas with Multiple Inputs and Multiple Outputs (MIMO) are used to improve wireless channel capacity [5]. For spatial diversity characteristics, the adopted MIMO technology provides an efficient, high data rate that is split into multiple lower-rate streams. Many wire-free communication technologies, such as WLAN, 3G, LTE, and WiMAX (4G), depend on MIMO antennas where many researchers developed with various shapes to cover a wide range of frequency bands [6].

Moreover, a MIMO antenna with a small size, high gain and performance, and CP radiation, as well as a large impedance bandwidth, is needed for many wireless communication systems [7]. Additionally, MIMO systems have been proposed to mitigate multipath fading effects [8], however, adjacent antennas coupling within a short separation distance may be the most significant drawback, especially in portable recent MIMO devices and systems [9].

In MIMO systems, this coupling must be reduced to improve antenna impedance matching and radiation properties [10], where mutual coupling

refers to electromagnetic losses caused by surface wave interactions between antenna elements [11]. Mutual coupling can be thought of as surface wave leakage in this case; however, it is highly dependent on antenna geometry, array structure, and separation distances [12].

II. Antenna Geometrical Details

The proposed antenna, see Figure 1, is constructed from circular patch geometry mounted on a Techtronic FR4 substrate. The antenna patch is fed with a coplanar waveguide (CPW) microstrip line printed on the same panel with the patch from the antenna substrate. The transmission line is designed as a Chebyshev transformer to maintain high coupling efficiency between the patch structure and the source over a wide frequency range [4]. The proposed transformer is designed based 3 stages (N) on the following relationship to be match with $Z_0 = 50\Omega$ SMA port [9] with input reflection coefficient of:

$$\Gamma(\theta) = Ae^{-2jn\theta}T_N(\sec\theta_m \cos\theta) = Ae^{-2j3\theta}T_3(\sec\theta_m \cos\theta), \quad (1)$$

$$\sec\theta_m \approx \cosh\left[\frac{1}{N}\cosh^{-1}\left(\left|\frac{\ln(Z_L/Z_o)}{2\Gamma_m}\right|\right)\right], \quad (2)$$

where Z_L is the load impedance, TM is m degree Chebyshev polynomial, $\Gamma_m = A$ is the reflection limit between each consecutive states which is assumed for this work as 0.05, and $\theta = \pi f/2f_0$.

For the proposed MTM structure, the array is oriented around the patch edges to suppress the surface waves in which an excellent enhancement can be achieved in terms of the antenna gain-bandwidth product [10]. The proposed array is constructed from eleven-unit cell that are distributed with a certain separation distance to achieve capacitive coupling effects that magnifies the electrical field fringing and return reduces the antenna size [4]. The individual unit cell is constructed from Hilbert curve fractal geometry

to maintain high surface current density within a limited area [3]. The frequency resonance of the individual unit cell can be tuned with a T-resonator structure through controlling the total impedance with a variable capacitor [9].

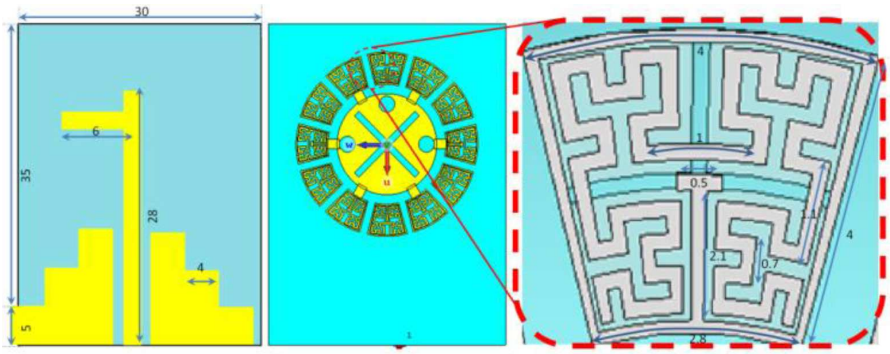

Figure 1. Antenna and MTM structures that are proposed in this work in mm scale.

III. MTM Characterizations

Now, to realize the performance of the proposed MTM unit cell, a numerical analysis is conducted based on CST MWS of a finite integral technique. The authors evaluated the proposed MTM unit cell S_{11} spectra using HFSS software package to be compared to their relative results from CST MWS. For this, a comparison study in terms of S-parameters spectra is presented in Figure 2. First of all, we found that the obtained results from both software packages agree very well to each other. Also, the frequency resonance is found to be very close to the frequency band of interest. This motivated the authors to consider this unit cell to be an excellent intimate to the proposed design that realizes an excellent reduction in the antenna surface waves from the patch edges [7]. The surface wave reduction is achieved by the effects of the proposed unit cell which suppresses the surface wave significantly at the frequency band of interest [9].

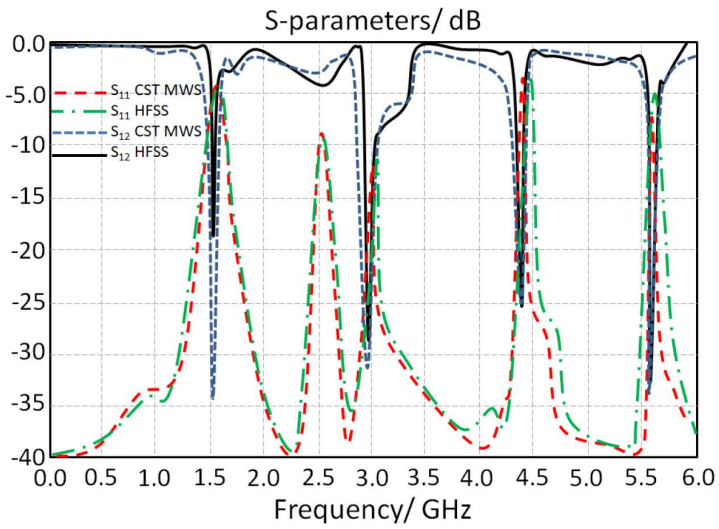

Figure 2. Evaluated S-parameters spectra from both considered software packages.

IV. Chebyshev Transformer

The proposed antenna structure is introduced to the proposed antenna to ensure bandwidth enhancement with maximum coupling. Moreover, the proposed CPW is structured with a Chebyshev transformer of three stages. Therefore, the authors, partially, studied the effects of the number of stages on the antenna bandwidth by varying the stage number from single stage to three stages as seen in Figure 3. It is observed that increasing the number of stages realizes a significant enhancement on the antenna bandwidth. This technique is invoked to maintain the antenna gain-bandwidth enchantments as shown in Figure 4. This is, in fact, achieved by eliminating the accumulated surface charges on the proposed CPW edges [8]. The charge accumulation is build up due to the steps of the proposed transformer [5]. Consensually trip the electromagnetic energy inside the substrate layer [6] that refers band with reduction by reducing the surface resistance of the patch to realize inconsistency between the load and the input impedance of

the source [2]. For this, the authors located the SMA port at certain direction for the proposed CPW which has significant effect of the antenna bandwidth. In this technique, the other side of the proposed CPW effect on discharging the accumulated surface charge indeed provides these enhancements [7].

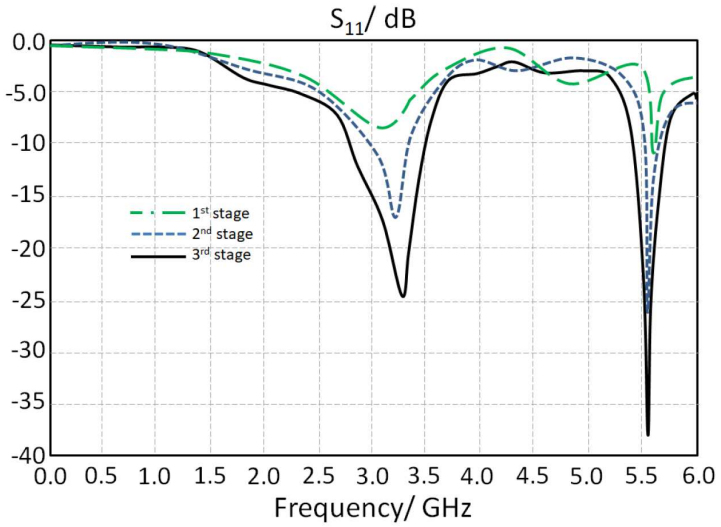

Figure 3. Evaluated S_{11} spectra based on the parametric study.

V. Design Methodology

The proposed antenna design methodology is presented in Figure 4 by considering a parametric flowchart. The optimal performance of the proposed antenna is characterized according to the antenna S-parameters. In this study, the parametric study is considered by changing the antenna substrate height (h), separation distance (G) between the antenna patch and the proposed MTM, and the cross width (w). These parameters are considered because they have significant effects on the antenna matching bandwidth and gain.

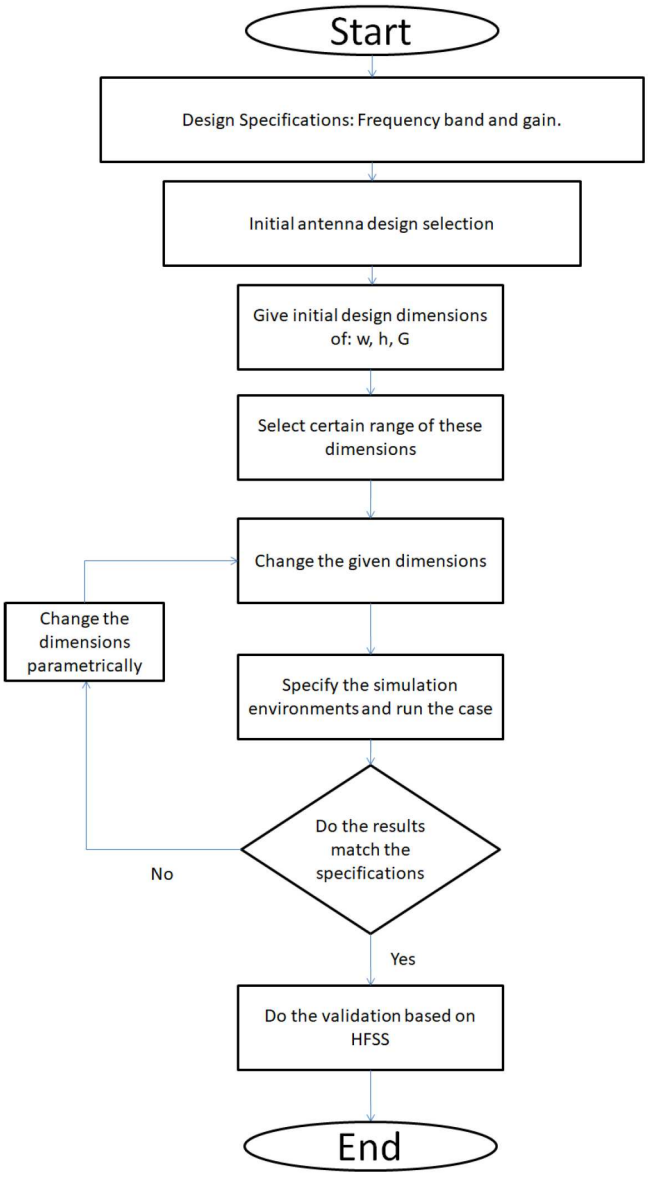

Figure 4. The considered design methodology flowchart.

It is studied numerically after combining the proposed MTM array to the proposed antenna circular patch. From the evaluated results in terms of S_{11} and gain spectra, see Figure 5, we found that the proposed antenna provides

a resonance mode around 3.35GHz with another band at 5.5GHz. These two frequency bands are very suitable for modern applications including 5G networks. Nevertheless, the antenna gain is found to be in the range of 2.2dBi at both frequency bands.

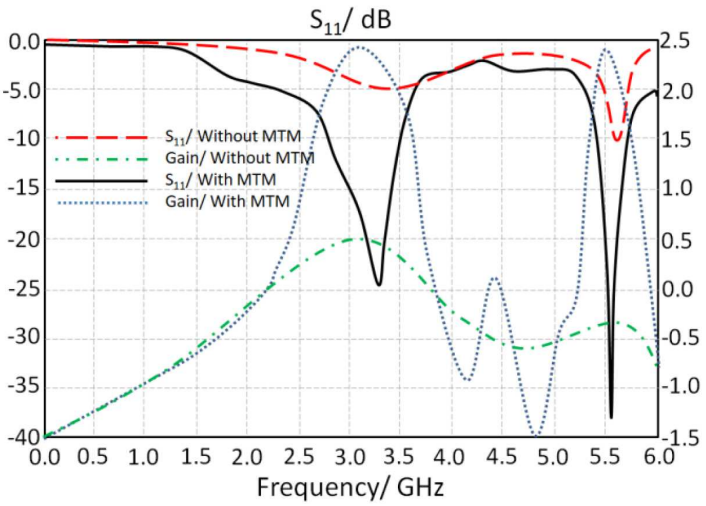

Figure 5. Evaluated antenna performance in terms of S_{11} and gain spectra.

Now, the design methodology is invoked to be *studied* parametrically using neural network architecture. For this network, the knowledge-based hybrid neural network (KBHNN) model is designed for the proposed antenna structure to suite sub-6GHz bands. In Figure 6, a synthesis model is defined as to obtain dimensions (G, W, h) of the antenna while providing the resonant frequency (F_r), gain (G_0), bandwidth (B.W.), quality factor (Q), and return loss spectra (S_{11}) at the input of the proposed KBHNN model.

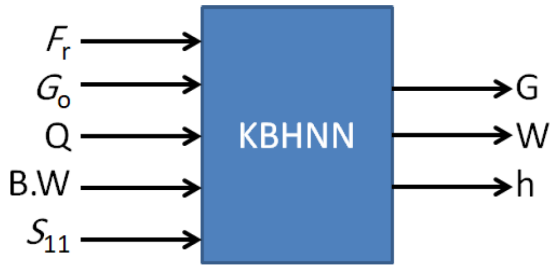

Figure 6. The synthesis of proposed antenna using KBHNN model.

Table I. Input antenna parameters

$G\times10^{-2}$/mm	$h\times10^{-2}$/mm	$W\times10^{-2}$/mm	F_{r1}/GHz	F_{r2}/GHz	$\lvert S_{11}\rvert$/dB	G/dB	Q/%	B.W./MHz
70	1	63	3.101	5.691	24.5	2.191	102	808
69	2	62	3.304	5.612	22.1	2.112	110	100
68	3	61	3.498	5.615	22.4	2.115	101	110
67	4	60	3.406	5.606	23.1	2.106	120	120
66	5	59	3.415	5.615	24.7	2.115	105	110
65	6	58	3.411	5.611	23.9	2.111	220	900
64	7	57	3.423	5.623	26.9	2.123	190	1000
63	8	56	3.493	5.693	28.1	2.193	108	110
62	9	55	3.491	5.691	28.4	2.191	210	120
61	10	54	3.403	5.603	22.8	2.103	310	101
60	11	53	3.409	5.609	22.3	2.109	190	191
59	12	52	3.408	5.608	25.3	2.108	102	709
58	13	51	3.421	5.621	27.2	2.121	101	910
57	14	50	3.411	5.611	22.9	2.111	103	802
56	15	49	3.456	5.656	26.3	2.156	107	905
55	16	48	3.416	5.616	23.1	2.116	105	596
54	17	47	3.482	5.682	22.9	2.182	100	608
53	18	46	3.474	5.674	23.0	2.174	199	499
52	19	45	3.391	5.591	23.1	2.291	106	120
51	20	44	3.398	5.598	23.1	2.098	113	110
50	21	43	3.392	5.592	23.9	2.092	160	103
49	22	42	3.409	5.609	24.1	2.109	101	903
48	23	41	3.406	5.606	23.9	2.106	132	170
47	24	40	3.041	5.601	22.4	2.211	171	171
46	25	39	3.422	5.622	22.4	2.122	127	408
45	26	38	3.433	5.633	27.3	2.133	117	705
44	27	37	3.424	5.624	27.9	2.124	149	588
43	28	36	3.411	5.611	24.1	2.111	101	190
42	29	35	3.401	5.610	27.8	2.11	103	498
41	30	34	3.413	5.613	27.4	2.113	102	793
40	31	33	3.391	5.591	26.3	2.091	210	100
39	32	32	3.394	5.594	25.6	2.094	207	605
38	33	31	3.392	5.592	26.1	2.092	131	807
37	34	30	3.409	5.609	25.3	2.109	199	406
36	35	29	3.401	5.601	25.9	2.101	107	609
35	36	28	3.405	5.605	25.2	2.105	102	204
34	37	27	3.489	5.689	24.2	2.189	101	129
33	38	26	3.488	5.688	23.4	2.188	190	110
32	39	25	3.477	5.677	24.4	2.177	109	798
31	40	24	3.409	5.609	27.8	2.109	102	620
30	41	23	3.401	5.161	27.3	2.11	101	290
29	42	22	3.412	5.612	27.0	2.112	109	440
28	43	21	3.495	5.695	24.9	2.195	104	890
27	44	20	3.496	5.696	25.2	2.196	105	901
26	45	10	3.479	5.679	25.1	2.179	108	504

It is worth noting that neural network models are an extremely versatile method for designing highly nonlinear devices. For this work, the conducted neural network is invoked to model the proposed antenna dimensions, including the distance between internal dimension data. Bandwidth (B.W), resonant frequency (F_r), gain (G), quality factor (Q), and S_{11} magnitude have all been used as input to the model as shown in Figure 6. As training data for the proposed network, about 50 samples are collected by varying the dimensions of the proposed microstrip patch antenna using the CST MWS software package, as shown in Table I. As will be shown later, these values are used to synthesis the proposed antenna.

The conducted KBHNN training loss results for the proposed synthesis are shown in Figure 7. It shows that 100 epochs are required for KBHNN training loss to get reduced from 100 to nearly 10^{-2}.

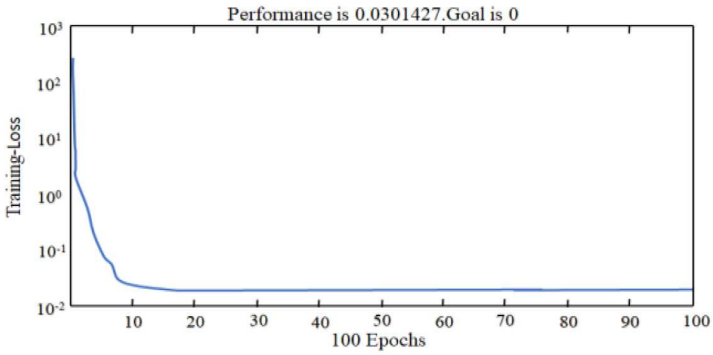

Figure 7. KBHNN training results for synthesis of microstrip patch antenna.

VI. Results Validation and Discussions

The obtained results are compared to those obtained from HFSS for validation before the fabrication process as will be seen later in the next section. The comparison reveals an excellent agreement between the considered software packages as seen in Figure 8. The antenna performance, in terms of S_{11} and gain spectra with radiation patterns are tested

numerically. The simulated S_{11} and gain spectra of the proposed antenna from both software packages are compared to each other. The obtained results are found to agree to each other excellently. It is found that the proposed antenna provides a bandwidth from 2.7GHz to 3.7GHz and 5.4GHz to 5.6GHz with gain of 2.2dBi at the frequency band of interest.

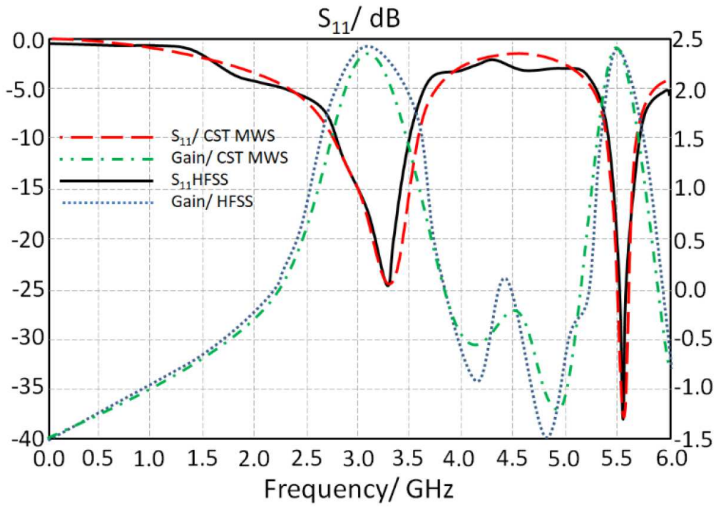

Figure 8. Antenna performance validation.

The antenna radiation patterns at 3.3GHz and 5.5GHz are presented in Figure 9(a). We found that the antenna radiation patterns are almost omni-directional around the antenna transmission line. This is due to the fact that the proposed antenna structure is designed without back panel ground plane [3]. Therefore, the surface current distribution on the antenna patch is distributed symmetrically as seen in Figure 9(b).

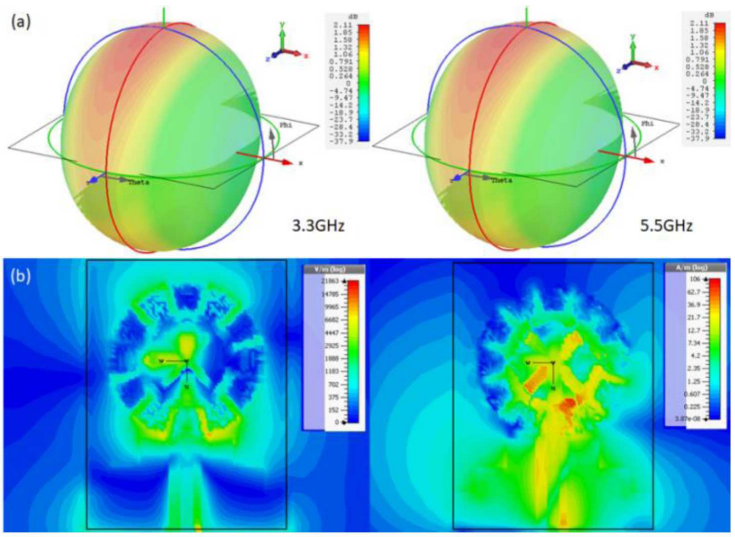

Figure 9. Antenna field distribution: (a) radiation patters and (b) surface current.

The proposed neural network model is applied for given F_r at 3.3GHz and 5.5GHz with $S_{11} \leq -16\text{dB}$ and a bandwidth of 0.6GHz to 0.65GHz with $G > 2\text{dBi}$. The antenna dimensions obtained through the network simulation model are summarized in Table II. It is seen that when the percentage errors are calculated and compared to the simulated ones, it seems that there is a very good fit corresponding to 0.044 percent error.

Therefore, according to the obtained dimensions, the proposed antenna performance is validated in another software package of HFSS simulator. The simulated results from both software packages show excellent agreement as seen in Figure 8 for S_{11} and gain spectra.

Table II. Obtained antenna dimensions from CST MWS and HFSS with respect to KBHNN model

Dimension/mm	CST	HFSS	KBHNN	Error
h	1	1.05	1.03	0.044
W	1.5	1.4	1.49	0.041
G	2.1	2.09	2.2	0.034

The proposed antenna is designed to realize a circular polarization feature at 3.3GHz and 5.5GHz as seen from the excel ratio (AR) in Figure 10. The evaluated results from both CST MWS and HFSS are compared to each other. It is found that the evaluated results agree very well to each other.

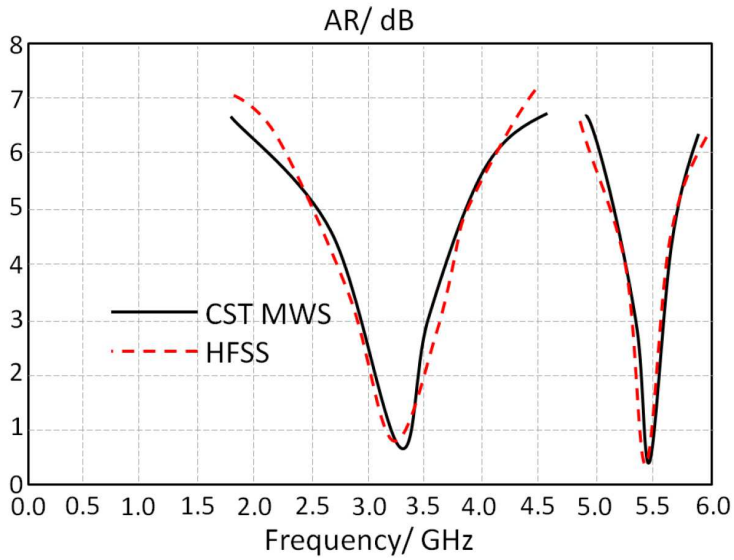

Figure 10. Antenna AR spectra validation.

Finally, the proposed antenna performance is compared to other published results in the literature as listed in Table III. It is found from such comparison that the proposed antenna system maintains a slow motion in the beam steering without the need for traditional switching process that requires biasing process.

On the other hand, in the proposed design, the beam steering process can be achieved from a single antenna element with single feed. This is found to be comparative property over the previous considered design in the literatures.

Table III. A comparison between the proposed antenna performance and other published designs

Ref.	Freq./GHz	Gain/dBi	Size (mm^2)
[6]	4.5-5.8	3.8-5	50×50
[8]	3.4/4.2	2/1.9	30×40
[9]	1.82/1.93/2.1	5.6/4.6/3.3	130×160
[10]	2.15/2.38	9	160.9×151.5
[11]	1.57-2.55	4.8	113×99
This work	2.7-3.7, 5.4-5.6	2.2	30×40

VII. Conclusion

The proposed antenna performance is numerically validated with respect to the proposed KBHNN results. It is found that the proposed antenna realizes a significant enhancement in the antenna matching impedance bandwidth. Such enhancement is achieved by introducing the proposed MTM unit cells. We found that the proposed antenna provides a bandwidth at two frequency bands 2.7GHz-3.7GHz and 5.4GHz-5.6GHz with gain of 2.2dBi. This is in fact attributed to the surface plasmon current motion on the antenna patch with a significant reduction in the surface waves. This is achieved when the proposed antenna structure is fetched to the patch structure. Therefore, the charge accumulation on the substrate is converted as plasmonic current on the patch surface. For this, the antenna bandwidth is improved through the proposed MTM introduction. Finally, it is found that the proposed antenna is an excellent candidate for the modern wireless communication networks.

References

[1] H. H. Al-Khaylani, T. A. Elwi and A. A. Ibrahim, A novel miniaturized reconfigurable microstrip antenna based printed metamaterial circuitries for 5G applications, Progress in Electromagnetics Research C 120 (2022), 1-10.

[2] M. N. N. Alaukally, T. A. Elwi and D. C. Atilla, Miniaturized flexible metamaterial antenna of circularly polarized high gain-bandwidth product for radio frequency energy harvesting, Int. J. Commun. Syst. 35 (2021), 122-131.

[3] A. Abdulmjeed, T. A. Elwi and S. Kurnaz, Metamaterial vivaldi printed circuit antenna based solar panel for self-powered wireless systems, Progress in Electromagnetics Research M 102 (2021), 181-192.

[4] A. I. Imran, T. A. Elwi and Ali J. Salim, On the distortionless of UWB wearable Hilbert-shaped metamaterial antenna for low energy applications, Progress in Electromagnetics Research M 101 (2021), 219-239.

[5] T. A. Elwi, A further realization of a flexible metamaterial-based antenna on nickel oxide polymerized palm fiber substrates for RF energy harvesting, Wireless Personal Communications 10(12) (2020), 1-15.

[6] Y. Alnaiemy, T. A. Elwi and L. Nagy, An end fire printed monopole antenna based on electromagnetic band gap structure, Automatika 61(3) (2020) 482-495.

[7] T. A. Elwi, Remotely controlled reconfigurable antenna for modern applications, Microwave and Optical Letters 6(1) (2020), 1-19.

[8] T. A. Elwi, Further investigation on solant-rectenna based flexible Hilbert-shaped metamaterials, IET Nanodielectrics 4(12) (2020), 1-12.

[9] T. A. Elwi and A. M. Al-Saegh, Further realization of a flexible metamaterial-based antenna on indium nickel oxide polymerized palm fiber substrates for RF energy harvesting, International Journal of Microwave and Wireless Technologies 5(4) (2020), 1-9.

[10] T. A. Elwi, D. A. Jassim and H. H. Mohammed, Novel miniaturized folded UWB microstrip antenna-based metamaterial for RF energy harvesting, International Journal of Communication Systems 1(2) (2020), 201-209.

[11] Y. Alnaiemy, T. A. Elwi and L. Nagy, Mutual coupling reduction in patch antenna array based on EBG structure for MIMO applications, Periodica Polytechnica Electrical Engineering and Computer Science 1(4) (2019), 1-11.

[12] R. K. Abdulsattar, T. A. Elwi and Z. A. Abdul Hassain, A new microwave sensor based on the Moore fractal structure to detect water content in crude oil, Sensors 21 (2021), 7143.